

PS Reconstruction of 3D Pore Space Using Multiple-Point Statistics Based on a 2D Training Image*

Yuqi Wu¹, Chengyan Lin¹, Lihua Ren¹, Weichao Yan¹, Yang Wang¹, and Songtao Wu²

Search and Discovery Article #42315 (2018)**
Posted December 10, 2018

*Adapted from poster presentation given at AAPG 2018 AAPG Annual Convention and Exhibition, Salt Lake City, Utah, May 20-23, 2018

**Datapages © 2018 Serial rights given by author. For all other rights contact author directly. DOI:10.1306/42315Wu2018

¹School of Geosciences, China University of Petroleum (East China), Qingdao, China (wuyuqi150348@163.com)

²Research Institute of Petroleum Exploration and Development, Beijing, China

Abstract

Macroscopic transport properties of porous media essentially rely on the geometry and topology of their pore space. The premise of predicting these transport properties is to construct an accurate 3D pore space. So far, the methods of modeling porous media are divided into two main groups, equipment imaging and stochastic statistical methods. The former method can acquire pore structure imaging using modern equipment such as X-ray computed tomography and laser scanning confocal microscopy, but the unavailability and the high cost of the equipment make their widespread application impossible. The latter methods, such as truncated Gaussian random field and simulated annealing methods, reconstruct 3D porous media based on some 2D thin sections by means of lower-order statistical functions. However, these functions cannot be able to reproduce the long-range connectivity of pore structure. Therefore, our research will present a stochastic technique of reconstructing 3D pore space using multiple-point statistics with the purpose of solving the proposed problems. The single normal equation simulation algorithm that serves as the simulation engine is the main tool to reproduce the long-range feature of pore space. In the simulation process, we took a 2D thin section as the training image for providing patterns of pore structure and extracted some pixels from it as the conditioning data. The extracted pixels must come from the centered region of a grain or pore, which can ensure the continuity of grain or pore among the adjacent layers to be simulated. To test the accuracy of the method, Berea Sandstone was used to test the method. Pore geometry and topology and transport properties of the reconstructed models were compared with those of the real model obtained by X-ray computed tomography scanning. The comparison result shows that reconstructed models are in good agreement with the real model obtained by X-ray computed tomography scanning in the two-point correlation function, the pore and throat size distributions, and single- and two-phase flow permeabilities, which verifies that the long-range connectivity of pore space can be reproduced by this method. Compared with other stochastic methods, a more accurate stochastic method of reconstructing 3D porous media is presented when only some 2D thin sections are available.

References Cited

Dong, H., and M.J. Blunt, 2009, Pore-Network Extraction from Micro-Computerized-Tomography Images: Physical Review E Stat Nonlin Soft Matter Phys, v. 80/3, 036307, 11 p. DOI:10.1103/PhysRevE.80.036307

Strebel, S., 2002, Conditional Simulation of Complex Geological Structures Using Multiple-Point Statistics: *Mathematical Geology*, v. 34/1, p. 1-21.

Valvatne, P.H., and M.J. Blunt, 2004, Predictive Pore-Scale Modeling of Two-Phase Flow in Mixed Wet Media: *Water Resources Research*, v. 40/7, W07406, 21 p. DOI:10.1029/2003WR002627

Reconstruction of 3D Pore Space Using Multiple-Point Statistics Based on a 2D Training Image

Yuqi Wu^{1*}, Chengyan Lin¹, Lihua Ren¹, Weichao Yan¹, Yang Wang¹, Songtao Wu²

1 School of Geosciences, China University of Petroleum (East China), Qingdao, China; 2 Research Institute of Petroleum Exploration and Development, Beijing, China. *E-mail address: wuyuqi150348@163.com



Abstract: Macroscopic transport properties of porous media essentially rely on the geometry and topology of their pore space. The premise of predicting these transport properties is to construct an accurate 3D pore space. So far, the methods of modeling porous media are divided into two main groups, equipment imaging and stochastic statistical methods. The former method can acquire pore structure imaging using modern equipment such as X-ray computed tomography and laser scanning confocal microscopy, but the unavailability and the high cost of the equipment make their widespread application impossible. The current latter methods, such as truncated Gaussian random field and simulated annealing methods, reconstruct 3D porous media based on some 2D thin sections by means of lower-order statistical functions. However these functions cannot be able to reproduce the long-range connectivity of pore structure. Therefore, our research will present a stochastic technique of reconstructing 3D pore space using multiple-point statistics with the purpose of solving the proposed problems. The single normal equation simulation algorithm that serves as the simulation engine is the main tool to reproduce the long-range feature of pore space. In the simulation process, we took a 2D thin section as the training image for providing patterns of pore structure and extracted some pixels from it as the conditioning data. The extracted pixels must come from the centered region of a grain or pore, which can ensure the continuity of grain or pore among the adjacent layers to be simulated. To test the accuracy of the method, Berea sandstone was used to test the method. We compare pore geometry and topology and transport properties of the reconstructed models with them of the real model obtained by X-ray computed tomography scanning. The comparison result shows that reconstructed models are good agreement with the real model obtained by X-ray computed tomography scanning in the two-point correlation function, the pore and throat size distributions, and single- and two-phase flow permeabilities, which verifies that the long-range connectivity of pore space can be reproduced by this method. Comparing with other stochastic methods, a more accurate stochastic method of reconstructing 3D porous media is put forward when only some 2D thin sections are available.

1 Introduction

Building a 3D porous medium for petroleum and environment engineers to obtain the transport properties and understand the fluid flow paths in the pore space. A novel idea of establishing pore space using multiple-point statistics (MPS) is proposed when only a 2D image is available.

2 Method

In 2000, Strebelle proposed Single Normal Equation Simulation (SNESIM) algorithm that effectively overcomes the problem of low simulation efficiency of previous MPS algorithms (Strebelle, 2002). SNESIM algorithm has been one of the most common methods for discrete variable simulation in MPS, such as sedimentary facies and pore space. The principle of this algorithm was introduced in detail by Strebelle (2002). Some key terms will be briefly described.

2.1 Data template and Data event

Data template, as well as search template, consists of central node u and n vectors radiating from the center node u . A data event is constituted by the data template and the n data values that are the data values of the n vectors.

2.2 Training image

A training image is essentially a conceptual model that tries to include all the pore-space structure patterns. For porous media modeling, the training image can be derived from the 3D model obtained by X-ray CT, or 2D slices. A 2D training image is being scanned by a 7×7 search template is shown in **Fig. 1**.

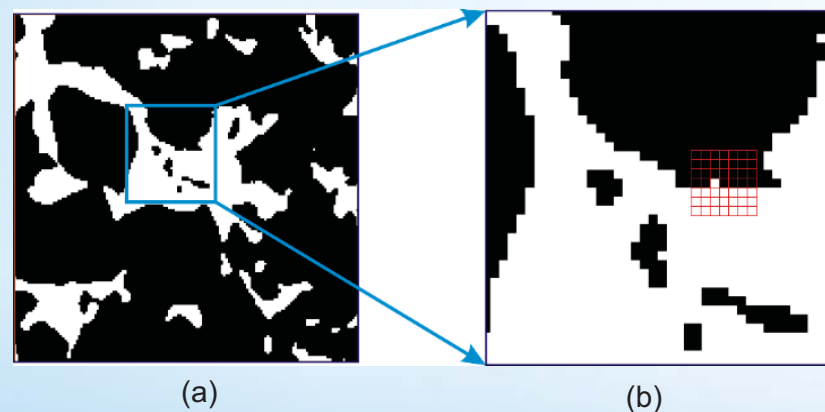


Fig. 1. (a) the training image derived from the 2D slice of Berea sandstone. (b) The training image is being scanned by a search template shown red grids.

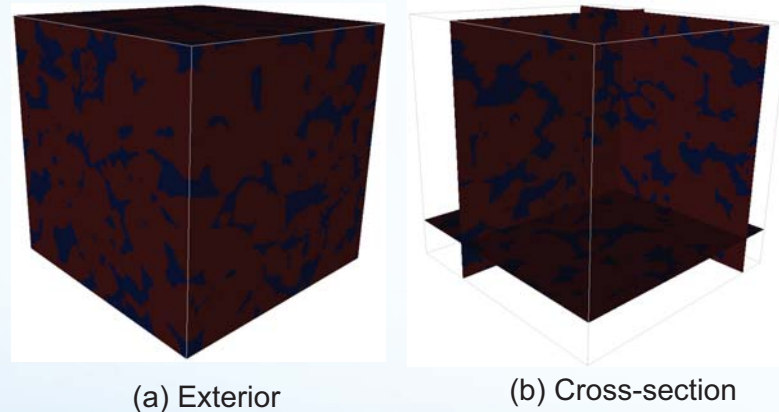


Fig. 2. Real model. The model obtained by X-ray CT is assumed to real model which will be used to compare with reconstructed models.

3 Reconstruction process of porous media

3.1 Test sample

The data of Berea sandstone was collected with a resolution of $5.345\mu\text{m}$ using X-ray CT (Dong and Blunt, 2009). The 3D images is exhibited in **Fig. 2**. As we all know, the model acquired by X-ray CT is approximately real, assumed as the real model.

3.2 Extraction of conditioning data

Three slices are randomly selected from the real model, shown in **Fig. 3**. A phenomenon can be observed among three layers that if a certain pore or grain is large enough in a layer, it will exist in adjacent layers. According to the aforementioned observation, we extract some pixels of large pores and grains from original image (**Fig.4a**) as the conditioning data (**Fig.4b**).

3.3 Procedure of reconstructing porous media

- (1) Set the original image as the first training image.
 - (2) Use four multi-grid template to scan the training image and build the search tree.
 - (3) Extract some pixels of large pores and grains from the training image to be conditioning data.
 - (4) Under the restraint of the conditioning data, simulate an unknown node and choose a certain state value of acquired from the search tree. The simulated pixel is added to conditioning data.
 - (5) A new image or layer will be generated when all the unknown nodes are simulated along the random path.
 - (6) Set the generated image as the new training image and renew the conditioning data. The step is the most one for the process.
- Loop (2)-(6) until a number of slices are generated.

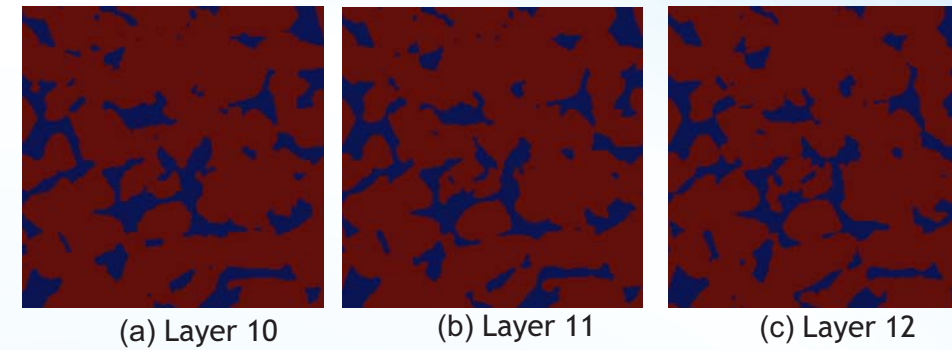


Fig. 3. Three slices selected from the real model. The viewpoint that a large pore tends to gradually change among adjacent slices is proved.

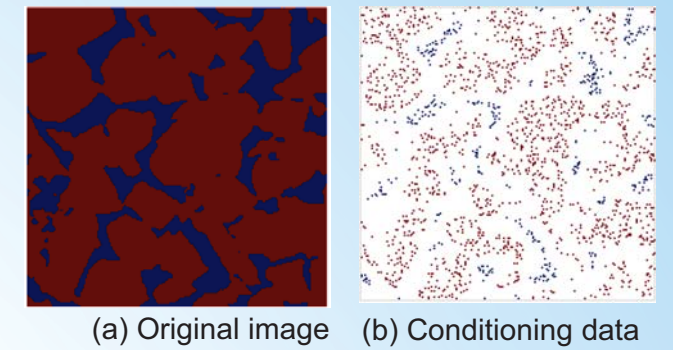


Fig. 4. Original image (a) and conditioning data (b).

4 Results and discussion

Based on the workflow of generating stochastic images, 199 slices are generated twice. Two stochastic 3D porous media have been reconstructed by stacking the original image and 199 slices according to the sequence of generating slices, shown in **Fig. 5** and **Fig. 6**.

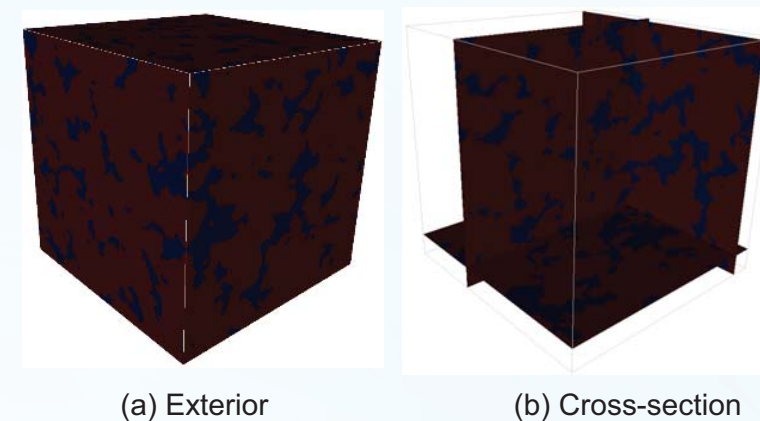


Fig. 5. Reconstructed model 1

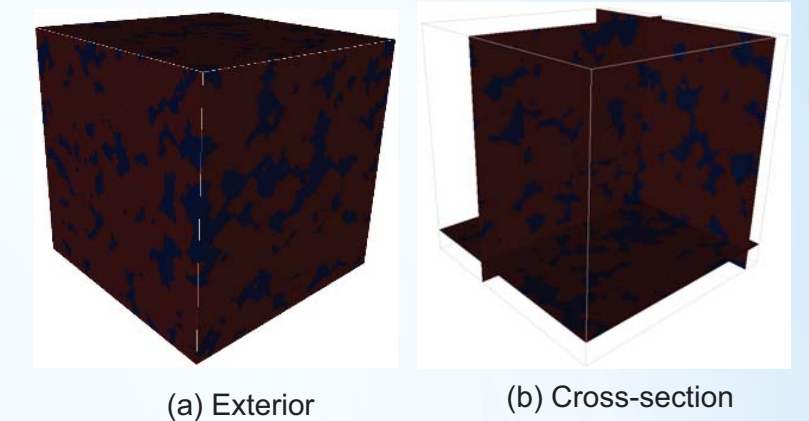


Fig. 6. Reconstructed model 2

To evaluate the accuracy of the reconstructed models, the comparisons of two-point correlation function, geometry and topology features of the pore space and the single-phase and two-phase flow properties between the real model and two stochastic reconstructions will be made.

4.1 Comparison on two-point correlation function

The function computes the probability of two voxels whose distance is h both in the pore space or grain. **Fig. 7** demonstrates that the two-point correlation function curves of reconstructed models compare well with that of the real model.

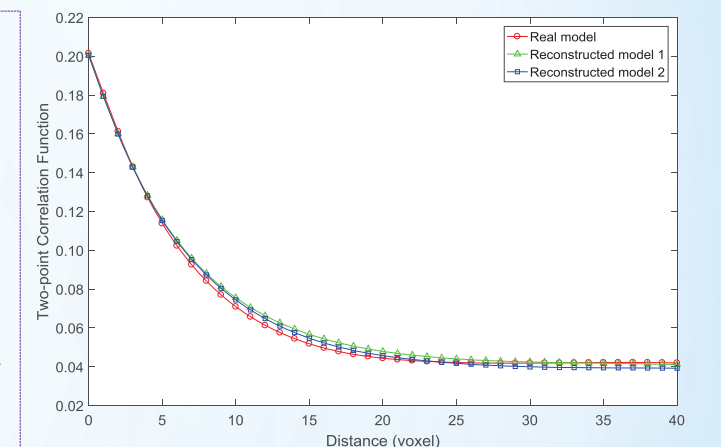


Fig. 7. Comparison of two-point correlation functions of the real model and reconstructed models

4.2 Comparison on geometry and topology features of pore space

The pore space can be divided into connected and isolated pore space in term of pore connectivity. The pore space distributions of the real model and two stochastic models are displayed in **Fig. 8**.

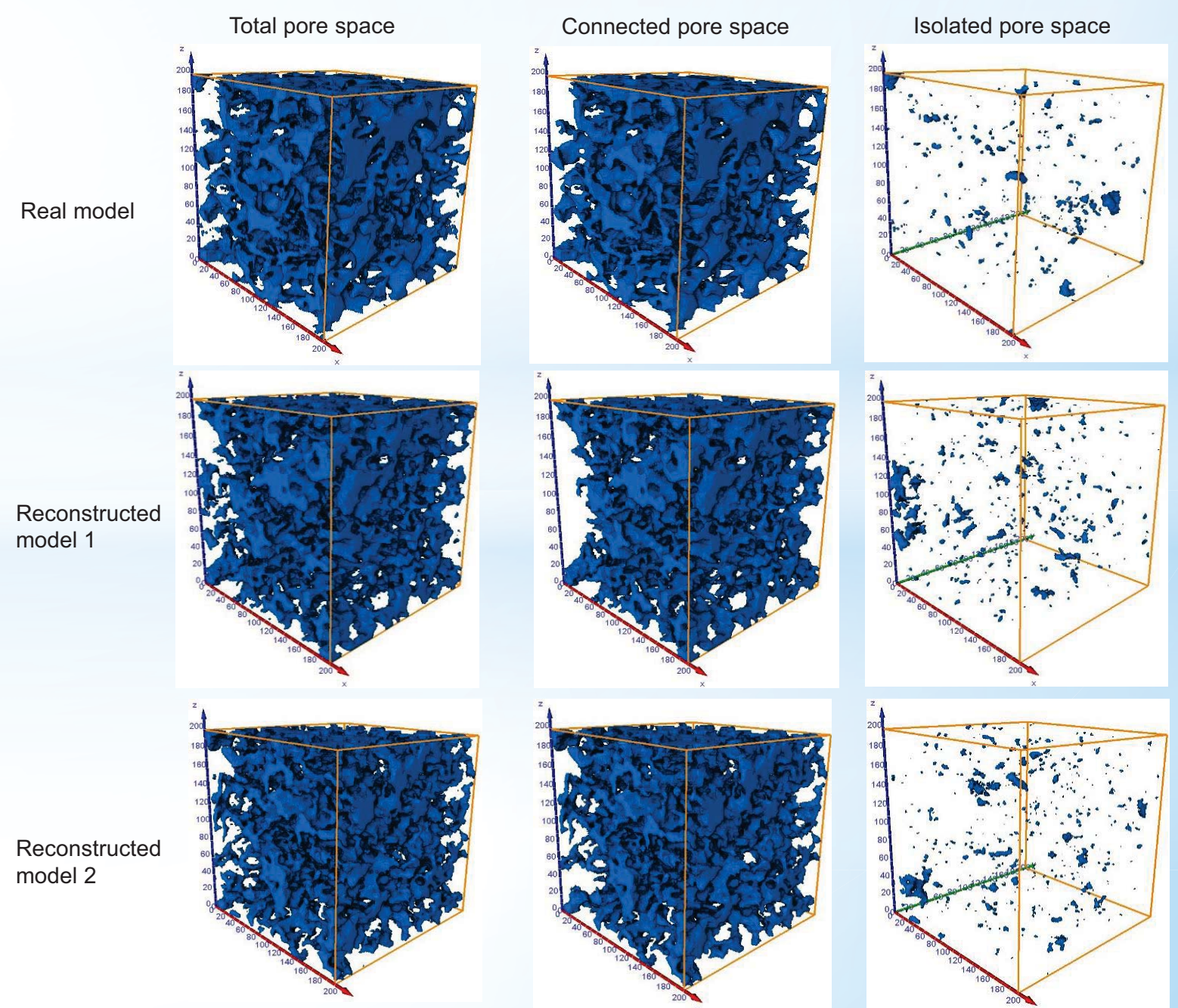


Fig. 8. Comparisons on pore space distribution of real model and reconstructed models

Reconstruction of 3D Pore Space Using Multiple-Point Statistics Based on a 2D Training Image

Yuqi Wu^{1*}, Chengyan Lin¹, Lihua Ren¹, Weichao Yan¹, Yang Wang¹, Songtao Wu²

1 School of Geosciences, China University of Petroleum (East China), Qingdao, China; 2 Research Institute of Petroleum Exploration and Development, Beijing, China. *E-mail address: wuyuqi150348@163.com



The maximal ball method (Dong and Blunt, 2009) is used to compute the geometry and topology parameters for pore space of three models, including pore and throat radius, shape factor, aspect ratio and coordination number as listed in **Table 1**. Besides comparisons of the specific values of the above parameters, the distributions of pore and throat radius, aspect ratio, pore and throat shape factor and coordination number are provided to further compare the geometry and topology of pore space in **Fig. 9**.

The pore network model of a porous medium can be generated by the maximal ball method. **Fig. 10** exhibits the pore network models of three images where the spheres represent pores and the tube columns represent throats.

On the whole, it is evident that the reconstructed models have similar pore-space structure characteristics with the real model.

4.3 Comparison on single-phase flow properties

Based on Navier-Stokes equation and Darcy's law, the numerical single-phase flow simulation is carried out on the real and reconstructed digital rock models. There are some assumed conditions that the flow process is steady-state, the fluid is incompressible Newtonian fluid and the fluid solid interface is no-slip. The fluid viscosity is set to 0.001Pa. S. According to the governing equations of single-phase fluid flow, the effective permeability in the Z axis direction of the real model and the stochastic reconstructions is calculated, shown in **Table 2**. It can be found that the effective permeability value of the real model approximates the experimental measured one. The permeability difference for three models is small. **Fig. 11** shows velocity field changes in pore space of three models when single-phase fluid flows through pore space. They are still similar.

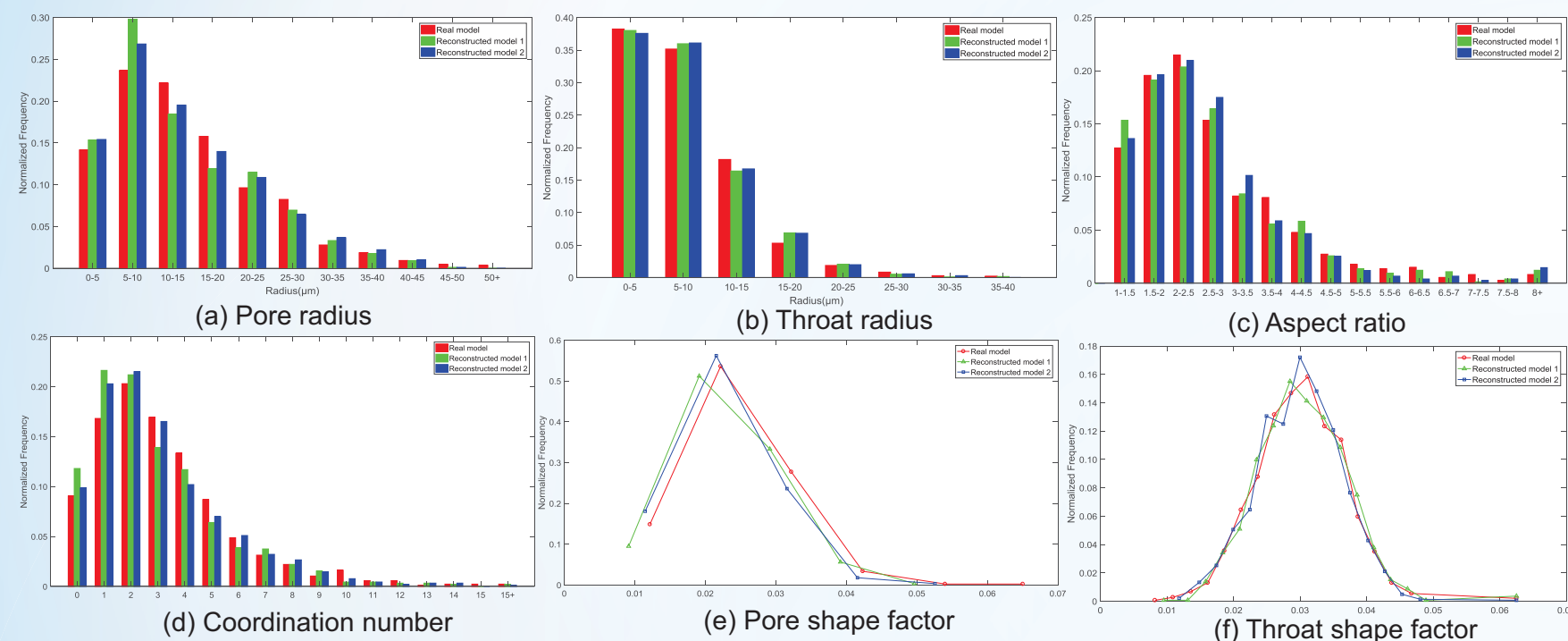


Fig. 9. Comparisons on distributions of pore-space geometry and topology parameters for the real model and reconstructed models

Table 1 Comparison of pore network structure parameters for the real model and the reconstructed models

Category	Real model	Reconstructed model 1	Reconstructed model 2
Porosity (%)	20.14	20.05	20.05
Total volume (μm^3)	246032557.91	244933107.55	244933107.55
Connected volume (μm^3)	237519831.41	231045400.36	229967694.68
Connectivity (%)	96.54	94.33	93.89
Centroid path tortuosity	2.05	2.02	1.97
Pore radius (μm)	Maximum	62.33	45.48
	Minimum	0.54	0.57
	Mean	14.44	13.58
Throat radius (μm)	Maximum	39.59	37.27
	Minimum	0.53	0.54
	Mean	7.56	7.47
Aspect ratio	Maximum	15.50	15.66
	Minimum	1.02	1.00
	Average	2.78	2.75
Pore shape factor	Maximum	0.0650	0.0496
	Minimum	0.0121	0.0091
	Mean	0.0243	0.0227
Throat shape factor	Maximum	0.0625	0.0625
	Minimum	0.0082	0.0095
	Mean	0.0300	0.0303
Coordination number	Maximum	19	19
	Minimum	0	0
	Mean	3.25	2.90

Table 2 Comparisons on effective permeability of the real model and reconstructed models

Category	Effective permeability $\times 10^{-3} \mu\text{m}^2$
Real model	1032.56
Reconstructed model 1	986.96
Reconstructed model 2	975.27
Experimental measure	1100

Table 3 Key parameters used for two-phase flow simulation of Berea sandstone

Water/oil surface tension ($\times 10^{-3} \text{N/m}$)	30
Water viscosity ($\times 10^{-3} \text{Pa}\cdot\text{s}$)	1.05
Oil viscosity ($\times 10^{-3} \text{Pa}\cdot\text{s}$)	1.39
Water resistivity ($\Omega\cdot\text{m}$)	1.2
Oil resistivity ($\Omega\cdot\text{m}$)	1000
Water density (kg/m^3)	1000
Oil density (kg/m^3)	900

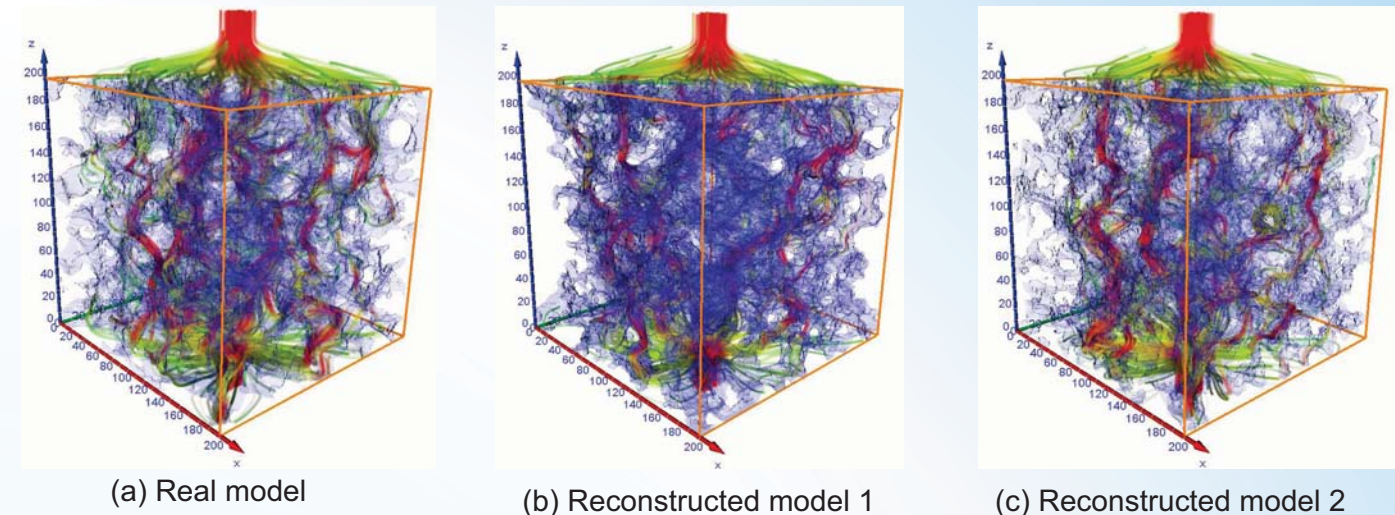


Fig. 11. Comparisons on velocity field change in pore space of three models for single-phase flow

4.4 Comparison on two-phase flow properties

We use the two phase code developed by Valvatne and Blunt (Valvatne and Blunt, 2004) to simulate primary drainage and imbibition based on the pore networks of the real model and reconstructed models. Some key parameters for two-phase flow simulation are set as listed in **Table 3**. The two-phase relative permeability curves of primary drainage and imbibition are computed and shown in **Fig. 12**. The relative permeability curves of reconstructed models agree well with that of real models regardless of oil flooding and water flooding, which further verifies the accuracy of the proposed method.

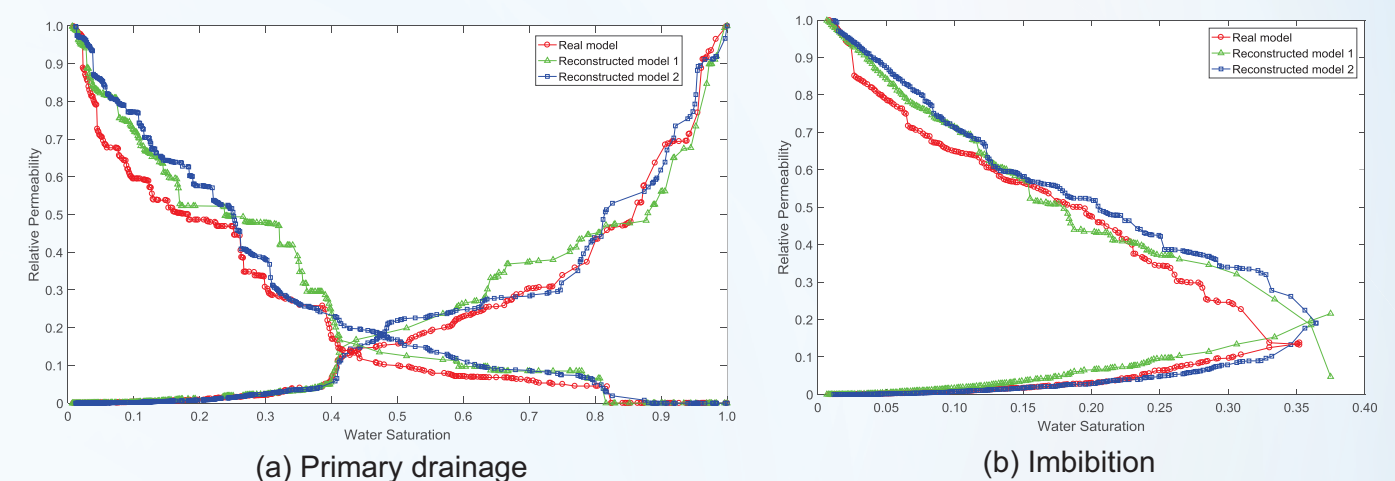


Fig. 12. Relative permeability curves of two-phase flow for the real model and reconstructed models

5 Conclusions

A 3D porous medium is the basis of petrophysics numerical experiment. In this paper, a method of reconstructing the porous media using multiple-point statistics based on a 2D image was presented. A 2D image was taken as a seed and a new 2D slice was generated. Then the new slice was set to the new training image to generate the next 2D image. The circle was repeated and many slices were generated layer by layer. Last the 3D stochastic models were reconstructed by stacking these slices. During the reconstruction process, the training image and conditioning data are anew updated when a new 2D slice is generated which ensures that the long-range connectivity of pore space can be reproduced in the porous media. The model established by X-ray CT is assumed as the real model. Then two-point correlation function and the parameters of pore-space geometry and topology features and single-phase and two-phase flow permeability are employed as the evaluation indexes. The comparisons of the indexes between the real 3D image and reconstructed 3D images were made. Last, it is proved that the reconstructed porous media are consistent with the real model in the pore-space features, for example long-range connectivity. These comparisons also verifies the reliability of the proposed method.

The presented reconstruction method provide a reliable tool to generate 3D model when a 2D image is available. If the computer has higher CPU and larger memory, the larger scale model can be reconstructed using MPS. Besides this, the method can be extended to apply reconstruction of multi-scale pore space for heterogeneous rocks.

Acknowledgments

This work is funded by Technology Major Project, P.R. China (grant number 2016ZX05054012) and Self-dependent Innovation Research Program of China University of Petroleum (East China) (grant number 18CX06024A). We would like to thank Branko Bijeljic from Imperial College London for providing the Berea sandstone data.

References:

- Dong, H., Blunt, M.J., 2009. Pore-network extraction from micro-computerized-tomography images. Phys Rev E Stat Nonlin Soft Matter Phys, 80(3 Pt 2): 036307.
- Strebelle, S., 2002. Conditional Simulation of Complex Geological Structures Using Multiple-Point Statistics. Mathematical Geology, 34(1), 1-21.
- Valvatne, P.H., Blunt, M.J., 2004. Predictive pore-scale modeling of two-phase flow in mixed wet media. Water Resour. Res. 40(7), W07406.

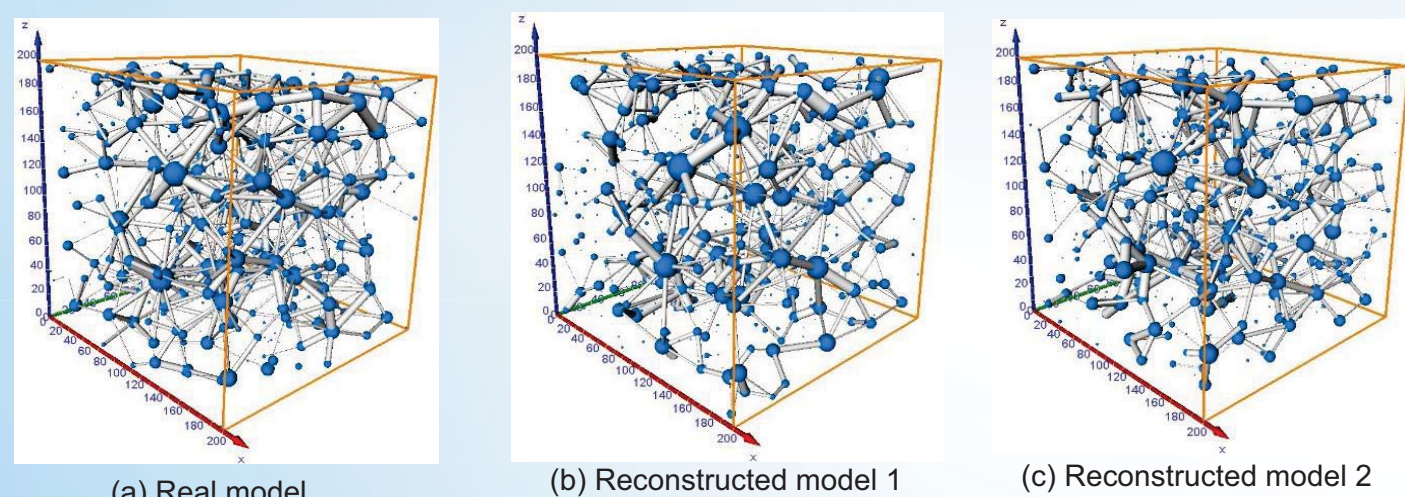


Fig. 10. Comparisons on pore network models of the real model and reconstructed models